

# Interaction of the Rattlesnake Toxin Crotamine with Model Membranes

Bruno A. Costa,<sup>†,¶</sup> Leonardo Sanches,<sup>‡,¶</sup> Andreza Barbosa Gomide,<sup>§</sup> Fernando Bizerra,<sup>||</sup> Caroline Dal Mas,<sup>†</sup> Eduardo B. Oliveira,<sup>⊥</sup> Katia Regina Perez,<sup>#</sup> Rosangela Itri,<sup>§</sup> Nancy Oguiura,<sup>‡</sup> and Mirian A. F. Hayashi<sup>\*,†</sup>

<sup>†</sup>Departamento de Farmacologia, Universidade Federal de São Paulo (UNIFESP), São Paulo 04044-020, Brazil

<sup>‡</sup>Laboratório Especial de Ecologia e Evolução, Instituto Butantan, São Paulo 05503-900, Brazil

<sup>§</sup>Departamento de Física Aplicada, Instituto de Física, Universidade de São Paulo (USP), São Paulo 05508-090, Brazil

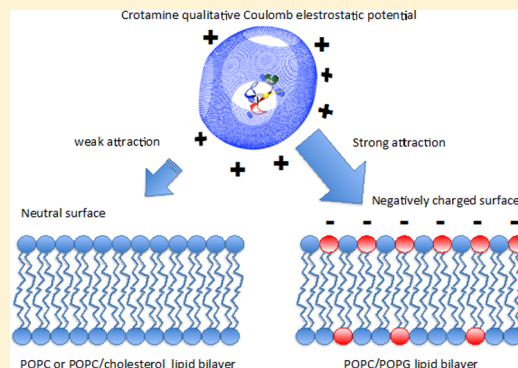
<sup>||</sup>Departamento de Medicina, Universidade Federal de São Paulo (UNIFESP), São Paulo 04021-001, Brazil

<sup>⊥</sup>Departamento de Bioquímica e Imunologia, Universidade de São Paulo, Ribeirão Preto, São Paulo, 14096-000, Brazil

<sup>#</sup>Departamento de Biofísica, Universidade Federal de São Paulo (UNIFESP), São Paulo 04021-001, Brazil

## S Supporting Information

**ABSTRACT:** Crotamine is one of the main constituents of the venom of the South American rattlesnake *Crotalus durissus terrificus*. A common gene ancestry and structural similarity with the antimicrobial  $\beta$ -defensins (identical disulfide bond pattern and highly positive net charge) suggested potential antimicrobial activities for this snake toxin. Although crotamine demonstrated low activity against both Gram-positive and Gram-negative bacteria, a pronounced antifungal activity was observed against *Candida* spp., *Trichosporon* spp., and *Cryptococcus neoformans*. Crotamine's selective antimicrobial properties, with no observable hemolytic activity, stimulated us to evaluate the potential applications of this polypeptide as an antiyeast or candidicidal agent for medical and industrial application. Aiming to understand the mechanism(s) of action underlying crotamine antimicrobial activity and its selectivity for fungi, we present herein studies using membrane model systems (i.e., large unilamellar vesicles, LUVs, and giant unilamellar vesicles, GUVs), with different phospholipid compositions. We show here that crotamine presents a higher lytic activity on negatively charged membranes compared with neutral membranes, with or without cholesterol or ergosterol content. The vesicle burst was not preceded by membrane permeabilization as is generally observed for pore forming peptides. Although such a property of disrupting lipid membranes is very important to combat multiresistant fungi, no inhibitory activity was observed for crotamine against biofilms formed by several *Candida* spp. strains, except for a limited effect against *C. krusei* biofilm.



## INTRODUCTION

Crotamine is a 42 amino acid polypeptide [YKQCHKKGG-HCFPKEKICLPSSDFGKMDCRWRWKCKKGSG], containing antiparallel  $\beta$ -sheets and a single  $\alpha$ -helix, stabilized by disulfide bonds (Cys<sup>4</sup>–Cys<sup>36</sup>, Cys<sup>11</sup>–Cys<sup>30</sup>, and Cys<sup>18</sup>–Cys<sup>37</sup>) and folded into a compact, amphipathic 3D structure.<sup>1–3</sup> Interestingly, defensins, which are members of a major family of antimicrobial peptides (AMPs), also show a similar fold and exactly the same disulfide bond pairings as crotamine.<sup>1–6</sup>

Many crotamine features have been described, including its ability to be internalized by mammalian cells, indicating that this peptide is a cell penetrating peptide (CPP),<sup>7</sup> with an exceptional specificity for actively proliferating cells,<sup>8–10</sup> which seems to be dependent on the presence of negatively charged proteoglycans on the cell surface.<sup>11</sup> In addition to the ability to carry nucleic acid into cells,<sup>11–13</sup> we demonstrated that the cytotoxic effects of crotamine are mediated through lysosomal

membrane permeabilization.<sup>14</sup> This stimulated us to also explore the antitumor activity of crotamine.<sup>9,15</sup> A number of recent studies describe natural peptides with both antimicrobial and antitumor properties, and the majority of them act mainly at the membrane level.<sup>16–21</sup>

Antimicrobial peptides (AMPs) are responsible for the first line of defense against invading microbes,<sup>22,23</sup> and one of the proposed mechanisms for their antimicrobial activity is the disruption of the cytoplasmic membranes.<sup>24–26</sup> For this reason, AMPs are perceived as a promising solution for the problem of microbial multidrug resistance.<sup>27</sup> Defensins are a group of AMPs found in different living organisms.<sup>28</sup> As mentioned, the common ancestry and similar 3D structure fold shared by

Received: December 4, 2013

Revised: April 22, 2014

Published: April 23, 2014

crotamine and  $\beta$ -defensins<sup>1,3,26,29</sup> led us to characterize the antimicrobial activity of crotamine against bacteria and several fungal species, including resistant clinical strains. The crotamine activity against Gram-positive and Gram-negative bacteria was mainly low, with the exception only of *Micrococcus luteus*, while a pronounced antifungal activity against *Candida* spp., *Trichosporon* spp., and *Cryptococcus neoformans* was observed.<sup>10,30</sup> Therefore, the important antifungal activity against either standard or clinical yeast strains suggested the potential of crotamine as a structural model compound for the development of a new generation of antifungal drugs with an unique capability to effectively fight against microbial resistance.

Although we cannot overlook the important toxic effects of crotamine previously described by others,<sup>31–33</sup> it is worth mentioning that these toxic effects are observed only for high doses of crotamine (usually hundreds of micrograms per mouse for a single dose). Because the cytotoxic and antifungal effects were observed *in vitro* at very low concentrations,<sup>10,14</sup> we have used low doses for the *in vivo* treatments (not exceeding 1  $\mu$ g per mouse per day), which were significantly below the LD<sub>50</sub> (ranging between 0.07 and 35.76 mg/kg; average  $\sim$ 6.9 mg/kg) described in the literature.<sup>29,33,34</sup> In this regard, under our conditions and employed protocols for our *in vivo* treatments, no important toxic effects have been observed by us so far.<sup>15</sup>

The specificity of AMPs for microorganisms in contrast to mammalian cells could be a consequence of their direct interaction with and subsequent permeabilization of microbial membranes.<sup>24,25</sup> In fact, it is well-known that bacterial membranes have a higher content of negatively charged lipids, while mammalian cell membranes, for example, those of erythrocytes, are mainly composed of zwitterionic lipids and cholesterol.<sup>35</sup> The use of vesicles with a defined composition of phospholipid is a powerful tool to conduct membrane perturbation studies. In this work, we made use of biomimetic membranes employing large unilamellar vesicles (LUVs) and giant unilamellar vesicles (GUVs) with different molar ratios of the zwitterionic lipid phosphatidylcholine (POPC) and the negatively charged lipid phosphatidylglycerol (POPG). The main purpose was to investigate the lipid membrane perturbation when in contact with the native crotamine dispersed in the outer vesicle solution. To assess the importance of the presence and the concentration of anionic lipid in the membrane composition to the antimicrobial activity of crotamine, the effect of peptide interaction on membrane stability was studied monitoring the 5,6-carboxyfluorescein (CF) leakage from LUVs composed of several POPC/POPG molar ratio. Optical microscopy of GUVs was also used to determine how crotamine interacts with membranes.

Crotamine displays a strong antiyeast and candidal effect, with no hemolytic activity and low harmful effects on normal (nontumoral) mammalian cells.<sup>10</sup> Accordingly, we have also evaluated the effect of crotamine against fungal biofilms, in which microorganisms form structured, coordinated, and functional communities that display a high level of antimicrobial resistance.<sup>36</sup>

## MATERIALS AND METHODS

**Materials.** The venom of *Crotalus durissus terrificus* was extracted from snakes maintained at the Faculdade de Medicina de Ribeirão Preto (FMRP) serpentarium, São Paulo University. The lipids POPC (1-palmitoyl-2-oleoyl-*sn*-glycero-3-phosphocholine), POPG (1-palmitoyl-2-oleoyl-*sn*-glycero-3-phospho-(1'-rac-glycerol) (sodium salt)), and cholesterol were pur-

chased from Avanti Polar Lipids (Alabaster, AL, USA). 5(6)-Carboxyfluorescein (CF) from Sigma-Aldrich (St Louis, MO) was purified as described.<sup>37</sup> Other chemicals and solvents were purchased from Sigma (Deisenhofen, Germany, or St. Louis, MO, USA).

**Preparation and Biochemical Characterization of the Native Crotamine.** Purification of native crotamine from snake venom was performed essentially as described elsewhere.<sup>13</sup> Briefly, 600 mg of crude dried venom was dissolved in 5 mL of 0.25 M ammonium formate buffer, pH 3.5, and the bulk of crotoxin, the major venom component, was eliminated by slow speed centrifugation as a heavy precipitate that formed upon slow addition of 20 mL of cold water to the solution. Tris-base (1 M) was then added dropwise to the supernatant to raise the pH to 8.8, and the solution was applied to a CM-Sephacrose FF (1.5  $\times$  4.5 cm<sup>2</sup>; GE Healthcare, Buckinghamshire, U.K.) column, equilibrated with 0.04 M Tris-HCl buffer, pH 8.8, containing 0.064 M NaCl. After the column was washed with 100 mL of equilibrating solution, crotamine was recovered as a narrow protein peak when the NaCl concentration of the eluting solution was raised to 0.64 M. The material was thoroughly dialyzed against water (benzoylated membrane, cutoff MW = 3000) and lyophilized. Amino acid analysis after acid hydrolysis of a sample (4 N MeSO<sub>3</sub>H + 0.1% tryptamine; 24 h at 115 °C) indicated a yield of 72 mg (14.7  $\mu$ mol) of crotamine and trace amounts of threonine, alanine, and valine (purity >98%).

Pure crotamine was then labeled with the Cy3-fluorescent dye as previously described using the Fluorolink Cyanine 3 (Cy3)-reactive dye (GE Healthcare).<sup>9,13</sup>

**Model Membrane Preparation. Large Unilamellar Vesicle (LUV) Preparation.** The POPC and POPG were dissolved in chloroform, which was evaporated under N<sub>2</sub> stream to deposit a thin lipid film on the wall of a glass tube. The final traces of residual solvent were removed under vacuum at room temperature for 1 h. Lipids were suspended in an appropriate amount of 50 mM CF dissolved in 10 mM HEPES, pH 7.4, to give a lipid concentration of approximately 25 mM. For the preparation of LUVs, the resulting multilamellar vesicle (MLV) dispersion was extruded using the Mini-Extruder system (Avanti Polar Lipids Inc., Alabaster, Alabama, USA), passing the MLV suspension through two-stacked polycarbonate membranes of 100 nm diameter pores. This process was repeated several times, and the free nonencapsulated CF was removed by chromatography on a Sephadex G25 medium (1.2  $\times$  20 cm<sup>2</sup>) column pre-equilibrated with 10 mM HEPES, pH 7.4, buffer with 150 mM glucose. The final phospholipid concentration of LUV suspensions was estimated for each preparation determining the total phosphorus content.<sup>38</sup> All liposomal preparations were freshly prepared and used in the same day.

**Giant Unilamellar Vesicle (GUV) Preparation.** The GUVs were prepared by the electroformation method. Briefly, 20  $\mu$ L of lipid in chloroform solution [2 mg/mL] was spread on the surfaces of two conductive glasses coated with fluor tin oxide, which were then placed with their conductive sides facing each other and separated by a 2 mm thick Teflon frame. This electro-swelling chamber was filled with 0.2 M sucrose solution, and it was connected to an alternating current of 2 V with a 10 Hz frequency for 2 h. The vesicle suspension was removed from the chamber and diluted into a 0.2 M glucose solution containing the desired amount of crotamine. The osmolarity of the sucrose and glucose solutions was measured with a Gonotec

030 cryoscopic osmometer (Osmomat, Berlin, Germany) before use, and they were carefully matched to avoid osmotic pressure effects. The vesicles were then immediately placed on the observation chamber. Due to the differences in density between sucrose and glucose solutions, the vesicles were stabilized by gravity at the bottom of the observation chamber.

**CF Efflux Experiments.** Experiments were performed with a fluorescence spectrophotometer F-2500 (Hitachi, Tokyo, Japan), using a fixed wavelength at 490 nm for excitation and 520 nm for emission. The temperature was kept at 25 °C. Both excitation and emission slits were set to 2 nm spectral bandwidth. The samples containing 100  $\mu$ M of lipids in 10 mM HEPES, pH 7.4, with 150 mM glucose were stirred continuously during the measurements. Crotonamine [5, 10, 20, or 40  $\mu$ M final concentration] was added to the cuvette, and the fluorescence signal was monitored during 2700 s. Then, a 100% reference point (corresponding to the total release of CF) was determined for each measurement by the addition of 20  $\mu$ L of a 10% (w/v) Triton X-100 solution followed by 300 s monitoring. The percentage of CF leakage was obtained using the following equation:

$$\text{leakage (\%)} = \frac{I_t - I_0}{I_T - I_0} \times 100$$

, where  $I_0$  and  $I_t$  correspond to the fluorescence intensity before and after the time ( $t$ ) of crotonamine addition, respectively.  $I_T$  is the fluorescence intensity after the addition of 10% Triton X-100 solution.<sup>39</sup>

**Optical Microscopy Observation and Experiments.** Vesicles were observed by using an inverted microscope Axiovert 200 (Carl Zeiss; Jena, Germany) in the phase contrast mode (Plan Neo-Fluar 63 $\times$  Ph2 objective (NA 0.75) and A-plan 10  $\times$  Ph1 (NA 0.25)) and fluorescence mode (103W Hg lamp, HXP 120, Kubler, Carl Zeiss, Jena, Germany). A Zeiss 43 HE filter set (excitation at 538–563 nm and emission at 570–640 nm) was used to observe the fluorescent dye Cy3 bound to crotonamine. Images were recorded with an AxioCam HSm digital camera (Carl Zeiss).

Two sets of experiments were performed. First, 100  $\mu$ L of GUV suspension prepared in 0.2 M sucrose was diluted into 600  $\mu$ L of either 2  $\mu$ M Cy3-labeled or 2–5  $\mu$ M nonlabeled crotonamine in 0.2 M glucose. Each sample was immediately placed on the observation chamber, and GUV morphological changes were observed along the time (63 $\times$  Ph2 objective). Quantification of a possible decrease in the GUV optical contrast due to changes in membrane permeability was performed using the ImageJ 1.46 software.

In the second set of experiments, the effect of nonlabeled crotonamine on GUVs was observed with a 10 $\times$  Ph1 objective. A representative observation field (A  $\times$  B, 2  $\mu$ m) was chosen and was recorded for 45 min. For each membrane composition, the lytic effect of 2  $\mu$ M crotonamine on GUVs was quantified by counting the fraction of GUVs that remains intact during the monitored period. The GUVs were manually counted, and only the vesicles larger than  $\sim$ 10  $\mu$ m were computed. All experiments were performed at room temperature (22–25 °C).

**Experiments with Biofilms.** Biofilms were produced, essentially as previously described,<sup>40</sup> using different *Candida* spp. isolates in polystyrene flat-bottomed 96-well microtiter plates (Techno Plastic Products, Switzerland). The used strains were *Candida albicans* ATCC 757 (clinical isolate), *Candida albicans* ATCC 997.5 (clinical isolate), *Candida krusei* ATCC

6258, *Candida parapsilosis* ATCC 22019, *Candida albicans* ATCC 90029, and *Candida glabrata* ATCC 90030. Briefly, the yeast isolates were grown at 37 °C for 18 h in RPMI 1640, pH 7.0 (Invitrogen-Gibco), and the cells were harvested and washed with phosphate buffered saline solution (PBS, IrvineScientific, Santa Ana, CA, USA) by centrifugation. Then a suspension of  $6 \times 10^4$  yeast cells in 100  $\mu$ L of PBD was placed in each well of a 96-well plate. The plates were incubated at 37 °C for 1.5 h, and the medium was aspirated. The nonadherent cells were removed by washing thoroughly three times with 200  $\mu$ L of sterile PBS, pH 7.2. Then, 150  $\mu$ L of RPMI 1640, pH 7.0, was added to each well, and the plates were incubated at 37 °C for 24 h. After this incubation period, the medium was aspirated again, and the nonadherent cells were removed once more by washing thoroughly three times with 200  $\mu$ L of sterile PBS, pH 7.2. Formed biofilms were treated with crotonamine [0.02–10.00  $\mu$ M] or with the positive control caspofungin [0.13–64.00  $\mu$ M] dissolved in 200  $\mu$ L of RPMI 1640, pH 7.0, for each well, during 48 h at 37 °C. Biofilm was quantified by 2,3-bis(2-methoxy-4-nitro-5-sulfo-phenyl)-2H-tetrazolium-5-carboxanilide (XTT)-reduction assay as described elsewhere.<sup>41</sup> A 100  $\mu$ L aliquot of XTT–menadione [0.1 mg/mL XTT, 1 mM menadione (Sigma Chemical Co.)] was added to each well, and the plates were incubated in the dark for 1.5 h at 37 °C, before spectrophotometric readings at 490 nm in a Spectramax M2e microplate reader (Molecular Devices; Sunnyvale, CA, USA). Experiments were carried out three times, in triplicate and on different days. The differences in biofilm metabolic activity among the isolates were compared by  $t$ -test analysis, and the significance level for  $p$  values is presented in the figures.

## RESULTS

Several antimicrobial peptides (AMPs) are able to destabilize membranes or to form pores, generally leading to leakage of the lipid vesicle or cell internal contents.<sup>42,43</sup> Studies conducted using large unilamellar vesicles (LUVs) with different phospholipid compositions [POPC or POPC/POPG (70:30 and 50:50 mol %)], containing the fluorescent dye carboxy-fluorescein (CF), allowed us to observe that crotonamine is not able to permeabilize neutral membranes since no leakage from POPC vesicles was observed in the experimental time (Figure 1A). However, it was possible to measure an increase of fluorescence due to the CF leakage, as a function of time, for membranes containing POPG, which provides a negatively charged surface in these model membrane vesicles (Figure 1B,C). Moreover, the lytic activity of crotonamine seems to be sensitive to POPG concentration in the membrane, as the extent of CF leakage from LUVs of POPC/POPG, 50:50 mol %, was higher (about 60% CF leakage) and faster compared with that observed for POPC/POPG, 70:30 mol % (about 23% CF leakage), for a similar peptide/lipid relationship and at same experimental period of time (Figure 1).

In order to unveil the mechanism involved in the LUV leakage caused by crotonamine, giant unilamellar vesicles (GUVs) were also used. Initial experiments dispersing GUVs in glucose solutions containing 5, 10, and 50  $\mu$ M crotonamine showed an extremely fast effect (data not shown). This effect was so quick that the interaction between the lipid bilayer and crotonamine could not be perceived under our monitoring conditions. Therefore, the current study was conducted focusing on the effects of 2  $\mu$ M crotonamine on GUVs with different compositions, that is, POPC/POPG, 75:25 mol %, POPC, and POPC/cholesterol (Chol), 90:10 mol %, intending to



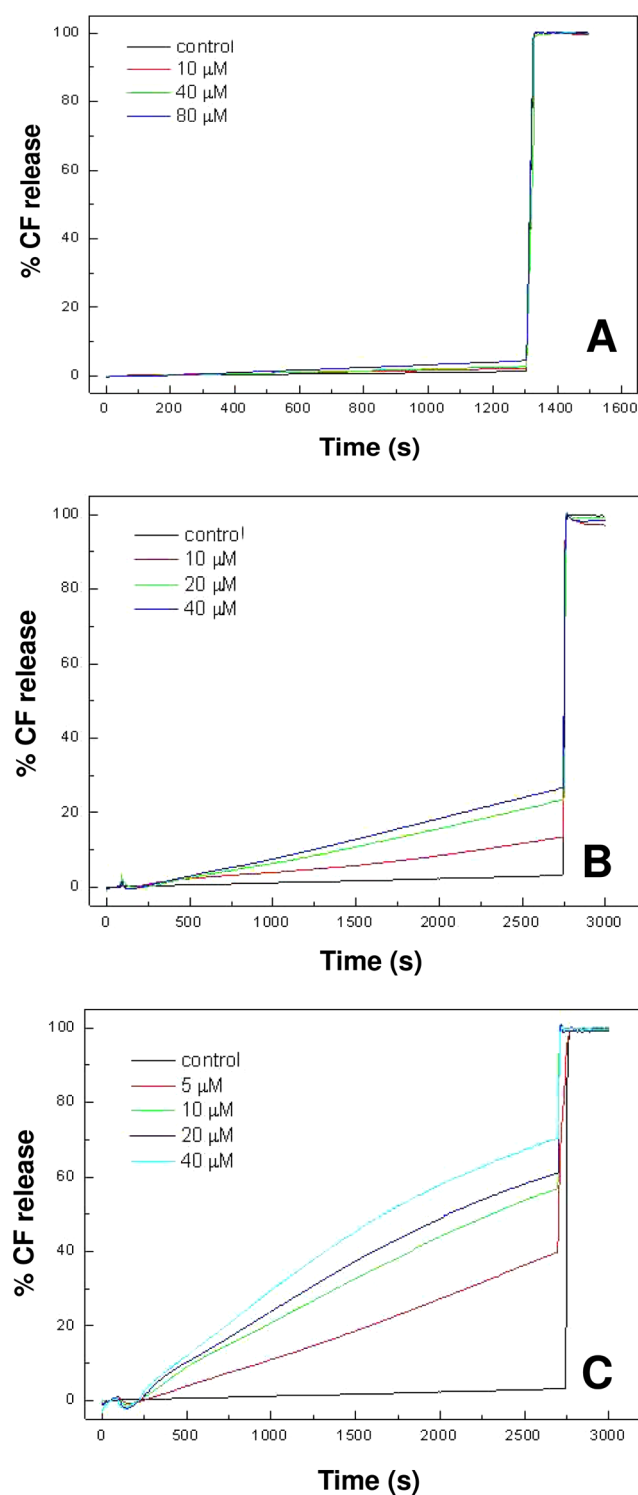


**Figure 1.** Time course of carboxyfluorescein (CF) leakage from large unilamellar vesicles (LUVs) with different compositions in the presence of varying amounts of crotonamine. This figure shows the time course of CF leakage of LUVs (%) composed by (A) POPC, (B) POPC/POPG, 70:30 mol %, and (C) POPC/POPG, 50:50 mol %, in the presence of increasing concentrations of crotonamine from 0 (control) up to 80  $\mu\text{M}$ .

model the bacterial and mammalian cell membranes charges, respectively. Figure 2 shows a GUV formed by POPC incubated with crotonamine, as an exemplary figure representing the common event observed with all vesicles of different lipid

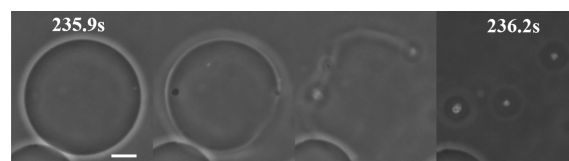


**Figure 2.** Phase contrast images from POPC giant unilamellar vesicles (GUVs) dispersed in an aqueous solution containing 2  $\mu\text{M}$  crotonamine. In the sequence of images, the membrane initially intact is drastically affected by crotonamine, followed by membrane disruption. Top number on the first and last images displays time in seconds (s). The moment of membrane addition to crotonamine solution is set as time 0 s. Scale bar spans 10  $\mu\text{m}$ .

composition. The GUVs formed only by POPC remained stable for more than 4–5 min in the presence of 2  $\mu\text{M}$  crotonamine, after which we observed a macropore formation followed by the lipid membrane bursting (Figure 2). Of note, this sequence of events was not preceded by nanopore formation or increase in membrane permeability to sugar exchange, which would lead to a loss of the membrane optical contrast.<sup>44</sup>

Aiming to better explore how the response of the membrane to crotonamine is influenced by the lipid composition, the lytic effect was then evaluated taking into account the percentage of vesicles that remained intact over time, after a period of incubation with a fixed concentration of crotonamine [2  $\mu\text{M}$ ]. Figure 3 shows the ratio of intact GUVs  $N_t/N_0$ , where  $N_0$

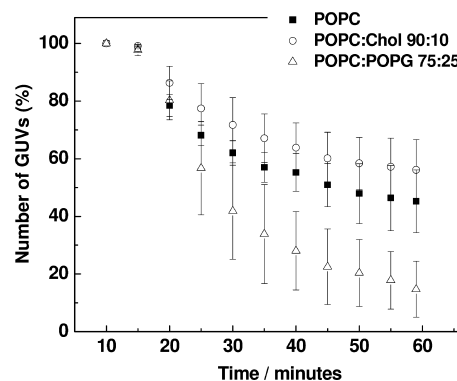


**Figure 3.** Time course of giant unilamellar vesicle (GUV) disruption. This graphic shows the percentage (%) of GUVs with distinct lipid compositions that remained intact after 1 h of incubation with crotonamine [2  $\mu\text{M}$ ]. This assay was performed by continuous observation under 10 $\times$  objective, which allows observation of a larger number of GUVs at the same time. Each experiment was performed in triplicate such that the behavior of *circa* of 100 GUVs was followed for each membrane composition. The error bars correspond to the mean deviation of three independent experiments.

corresponds to the number of GUVs on the observation screen at the initial time (10 min of incubation) of video-recording and  $N_t$  is the number of GUVs that remained on the screen in the time course of the experiment. As one can note, the lipid composition plays an important role in the membrane–crotonamine interaction. For membranes composed only of POPC, about 50% of GUVs are destroyed after 1 h in the presence of 2  $\mu\text{M}$  crotonamine. The presence of Chol in the POPC membrane partially hinders the membrane disruption. On the other hand, the presence of anionic lipid POPG in the membrane enhances the crotonamine effect, such that only 10% of GUVs remained intact after 1 h (Figure 3). It is important to

mention here that the presence of Chol does not preclude the effect of crotonamine on the membrane, since membrane disruption is still observed, although to a lower extent (Figure 3), suggesting that Chol may contribute to protecting the POPC-based membrane from crotonamine action. On the other hand, the presence of ergosterol in the POPC/POPG vesicles does not protect the membrane from crotonamine action (see Supporting Information).

GUVs formed by POPC/POPG, 75:25 mol %, were monitored for up to 30 min in the presence of 2  $\mu\text{M}$  of fluorescent labeled Cy3-crotonamine, during which we observed initially a homogeneous distribution of the fluorescence in the vesicle lipid membrane (Figure 4). After a period of toxin–

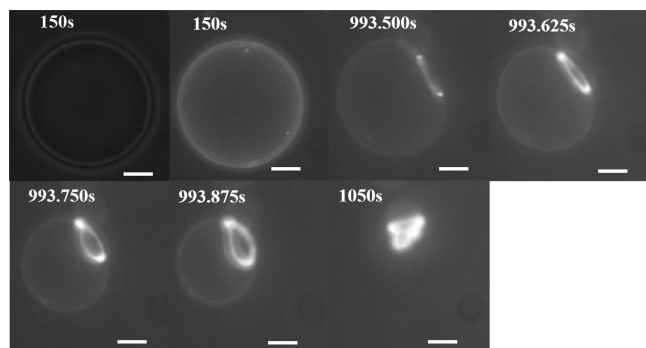


**Figure 4.** Cy3-labeled crotonamine [2  $\mu\text{M}$ ] distribution on giant unilamellar vesicles (GUVs) composed of POPC/POPG (75:25) allowed observation of the formation of the macropore and the subsequent membrane shrinking and bursting. The first panel shows a phase contrast image photo at 150 s, while the subsequent photos are fluorescent image snapshots. Top numbers on the images display time in seconds (s). The moment of membrane addition to labeled-crotonamine solution is set as time 0 s. Scale bar spans 10  $\mu\text{m}$ .

membrane contact, Cy3-labeled crotonamine molecules are found preferentially in a membrane region forming a macropore. Such a macropore formation is thus coupled to membrane instability, which leads to the vesicle shrinking, due to the content leakage, and bursting of the lipid membrane afterward (Figure 4). Considering the increase of the fluorescence intensity of the pore-containing membrane, one can suggest that not all crotonamine bound to the lipid participates in the pore formation.

Multidrug resistance is the main cause of concern for the treatment of infectious diseases caused by bacteria and fungi. Several studies have suggested the roles in multidrug resistance of biofilms, in which the pathogen resides inside a protective coat made of extracellular polymeric substances, directly influencing the virulence and pathogenicity of a pathogen.<sup>45</sup> Therefore, considering the antifungal activity of crotonamine against several *Candida* spp. strains<sup>10</sup> and its ability to interact with negatively charged lipid membranes shown here, the effect of crotonamine on biofilms formed by *Candida* spp. strains [namely, *Candida albicans* ATCC 757 (clinical isolate), *Candida albicans* ATCC 997.5 (clinical isolate), *Candida krusei* ATCC 6258, *Candida albicans* ATCC 90029, and *Candida glabrata* ATCC 90030] was also evaluated. Although significant antifungal activity has been demonstrated for crotonamine against several *Candida* spp. strains (MIC ranging from 12.5 to 50.0  $\mu\text{g/mL}$ , which correspond to 2.5–10.0  $\mu\text{M}$ ),<sup>10</sup> no significant activity on biofilms could be observed under the conditions employed here. The only exception was for the biofilms formed by *C. krusei* (ATCC 6258), for which only a limited effect could

be observed at higher concentrations of crotonamine [i.e., 10  $\mu\text{M}$ ] (Figure 5). The higher sensitivity of *C. krusei* to crotonamine

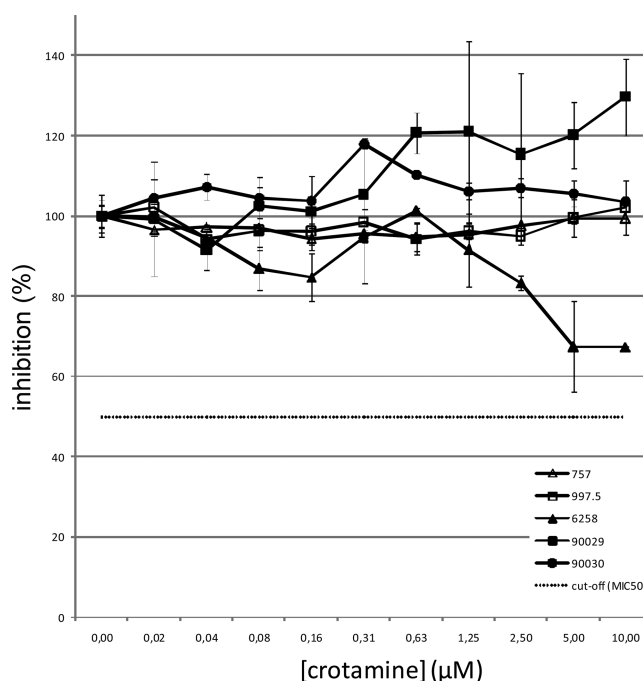


**Figure 5.** Effect of crotonamine on biofilms formed by different strains of *Candida* spp. Effects of increasing concentrations of crotonamine on biofilms formed by *Candida albicans* ATCC 757 (clinical isolate), *Candida albicans* ATCC 997.5 (clinical isolate), *Candida krusei* ATCC 6258, *Candida albicans* ATCC 90029, and *Candida glabrata* ATCC 90030 are shown. The dotted line indicates MIC<sub>50</sub>. Each experiment was performed in triplicate.

(MIC value ranging from 2.5 to 5.0  $\mu\text{M}$ )<sup>10</sup> may be due to the slight but significant differences in its membrane composition compared with those of *C. albicans* or *C. glabrata*.<sup>46</sup>

## DISCUSSION

We used unilamellar bilayers with controlled lipid composition to analyze how crotonamine interacts with lipid membranes. The results demonstrated that crotonamine acts to a higher extent on negatively charged membranes than on zwitterionic membranes, with or without cholesterol (Chol) (Figures 1–3). Noteworthy, in the same way as proteins from the  $\beta$ -defensin family, crotonamine presents a high positive net charge on the surface.<sup>2</sup> This facilitates its binding to negatively charged surfaces driven by electrostatic interaction, as observed for other antimicrobial cationic peptides, which are dependent on the interaction with the negatively charged components present on the outer bacterial envelope.<sup>23</sup>

The analysis of GUVs also revealed that crotonamine exhibits a similar lytic mechanism (Figures 2 and 4) to a greater or lesser extent depending on the anionic lipid POPG amount in the membrane. Membrane disruption is caused by the perturbation of a significant portion of the membrane bilayer, followed by a quick release of the inner solution and the complete burst of the giant vesicle. Crotonamine destabilizes the membranes without being preceded by the formation of stable pores smaller than the optical resolution of the microscopy (below a few micrometers), since no gradual decrease of optical contrast of vesicles was observed. Bursting of membranes has been also reported under the action of other bioactive molecules such as

gomesin<sup>47</sup> and detergents.<sup>48</sup> Interestingly, the macropore formation could be pictured by using fluorescently labeled crotonamine, which also demonstrated that not all crotonamine is recruited to form the pore through which the inner content leaks (Figure 4). The data for LUVs and GUVs composed of POPC/Chol also corroborate our previous report of low cytotoxicity of crotonamine for nontumoral cells, which have fewer negatively charged proteoglycans on the cell surface, and the lack of hemolytic activity.<sup>15,10</sup> They both must be dependent on the neutral charge of the model vesicles and the presence of cholesterol, which confers a lower interaction of crotonamine and higher membrane rigidity, because slower and less effective disruption of vesicles was observed (Figures 1–4). In a recent paper, Sieber and co-workers proposed a homo-oligomeric pore formation in planar bilayers of a lipid mixture from aolectin, a mixture of lipid that also has negatively charged lipids.<sup>49</sup> However, these authors employed a bath solution containing 1 M KCl, which is intrinsically necessary for this type of experiment. The use of such a high amount of salt may screen the charges of both membrane and polypeptide, thus resulting in a different mechanism of crotonamine insertion into the membrane. Furthermore, the authors also indicated no pore-forming activity for bath solutions containing only 100 mM CaCl<sub>2</sub>. It is also of worth mentioning here that we have demonstrated previously that 12.5 mM NaCl can inhibit the antibacterial activity of crotonamine.<sup>29</sup> Therefore, in the current paper, the experiments were conducted in the absence of salt, under such condition that the charges of crotonamine and lipid membrane are expected to be freely accessible.

Our GUV experiments showed that, in a first step, crotonamine is homogeneously distributed over the entire vesicle surface (Figure 4). We may hypothesize that positively charged crotonamine initially bound to the lipid bilayer exerts anionic lipid clustering in the membrane surface (Figure 6); this

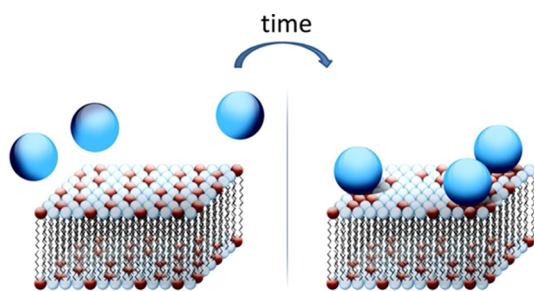


**Figure 6.** Interaction of crotonamine with POPC/POPG lipid bilayer. Graphical representation of the time evolution of crotonamine (blue balls) interacting with the lipid membrane composed of POPC (white lipid head) and POPG (red lipid head). The light blue face indicates the neutral face of crotonamine, while the dark blue face represents the positively charged region of crotonamine, which preferentially interacts with the negative charge of the POPG (red lipid head), inducing lipid demixing.

interaction, by turn, may favor the accumulation of crotonamine on a limited membrane region, causing its destabilization that ends in membrane rupture. The assemblage may create a macropore that compromises the membrane integrity, leading to its rupture and vesicle bursting. More studies are still necessary to elucidate how crotonamine anchors on the lipid membrane and whether lipid demixing driven by electrostatic interaction takes place. Finally, crotonamine may be considered another example of a natural peptide with antibacterial action in

which ionic attraction is of utmost importance followed by reorientation of lipids as also reported for other AMPs.<sup>50</sup>

Molecular dynamics simulation studies suggested that defensins act in a dimeric form to disrupt membranes, explaining how the individual structures of the defensins are responsible for their different actions on microbes.<sup>51</sup> In fact, it has been proposed that defensins exhibit their activity by disrupting bacterial membranes as a result of oligomer formation, because their antimicrobial activity and the ability to form dimers in solution appear to be directly proportional.<sup>52,53</sup> It was also demonstrated that aggregation of oligoarginines leads to partial disruption of the bilayer integrity due to the accumulated large positive charge at its surface, which increases membrane–surface interactions due to the increased effective charge of the aggregates.<sup>54</sup> Interestingly, at high concentrations, crotonamine may also oligomerize in aqueous solution as demonstrated by others.<sup>49,55,56</sup> However, in aqueous solutions and under our conditions of purification, due to the high hydrosolubility of native crotonamine, only a single peak was observed by MALDI-TOF mass spectrometry (data not shown), which suggests that the crotonamine was monomeric in solution under our study conditions, different from those employed by others.<sup>49</sup>

Furthermore, the preferential antimycotic activity *in vitro*<sup>10</sup> may be explained by the higher affinity of crotonamine for the charged lipid membrane, because each fungal strain has also variable membrane composition,<sup>57–59</sup> and the presence of ergosterol seems to not hamper this affinity, as demonstrated here (Supporting Information).

Because the surface-attached communities called biofilms represent a survival strategy employed by the microorganisms to increase their resistance to the antifungal drugs and stress imposed by the environment<sup>60,61</sup> and considering the ability of crotonamine to disrupt lipid cell membranes, we evaluated its effects on biofilms formed by several *Candida* spp. strains. Microorganisms growing in a biofilm are highly resistant to antimicrobial agents by one or more mechanisms, and the microorganisms forming biofilms are approximately 10 to 1000 times more resistant to the antibiotics than the planktonic cells.<sup>60,62</sup> Biofilms can be formed by Gram-positive and Gram-negative bacteria and mainly by fungus.<sup>61</sup> The most frequently described fungus in clinics is the *Candida* spp., of which *C. albicans* represents the most frequently isolated species.<sup>61,63</sup> It is also important to remark that although the lipid membrane composition was shown to vary significantly between each strain of *Candida* spp., as demonstrated for the planktonic form,<sup>64</sup> these differences in lipid composition did not allow us to explain the relative lower MIC value determined for crotonamine against some of the *Candida* spp. strains studied.<sup>10</sup> More recently, lipidomic studies showed that *C. albicans* biofilms contain higher levels of phospholipid and sphingolipids than planktonic cells and that the ratio of PC to PE is lower in biofilms compared with planktonic cells.<sup>64</sup> Therefore, aiming to explore the potential activity of crotonamine on biofilm formed by different strains of *Candida* spp., we conducted here assays that did not allow observation of any significant effect, even using high concentrations of this native peptide [up to 10  $\mu$ M] (Figure 5), which corresponds to about two times the MIC value.<sup>10</sup> Despite the higher activity of crotonamine against planktonic fungus,<sup>10</sup> its weak activity against biofilms only for *C. krusei* could sound disappointing at first. However, we believe that the importance of lipid charge for crotonamine interaction demonstrated here, as well as its ability to



destabilize lipid membranes to promote the release of the inner content, in the similar way as described for the lysosomes,<sup>14</sup> will greatly contribute to further exploration of its biotechnological and medical applications.

It should be remarked, however, that under certain conditions, crotonamine and derived peptides are able to internalize through mimetic membranes without disrupting the membrane.<sup>65</sup> Therefore, it is reasonable to imagine that besides the lipid membrane disruption activity, crotonamine might also have putative intracellular targets to be discovered in microorganisms, as we have recently described for mammalian cells.<sup>14</sup>

Given the ability of crotonamine to form complexes with genes and also to carry them and potentially other therapeutic molecules into cells,<sup>11,13,12</sup> we believe that the antimicrobial activity of crotonamine could be improved by exploring the cell delivery properties of this peptide. Thus, the association of therapeutic antibiotics or killer genes with crotonamine, aimed at targeted transport, might contribute to the development of a new generation of antifungal drugs that could effectively solve the growing problem of microbial resistance.

## ■ ASSOCIATED CONTENT

### ■ Supporting Information

Time course of giant unilamellar vesicle (GUV) disruption. This material is available free of charge via the Internet at <http://pubs.acs.org>.

## ■ AUTHOR INFORMATION

### Corresponding Author

\*Prof. Mirian A. F. Hayashi, Ph.D. Mailing address: Departamento de Farmacologia, Universidade Federal de São Paulo (UNIFESP), Rua 3 de maio 100, Ed. INFAR, 3rd floor, CEP 04044-020, São Paulo, Brazil. Tel: +55-11-5576 4447. Fax: +55-11-5576 4499. E-mail: [mhayashi@unifesp.br](mailto:mhayashi@unifesp.br) or [mhayashi.unifesp@gmail.com](mailto:mhayashi.unifesp@gmail.com).

### Author Contributions

<sup>†</sup>B.A.C. and L.S. contributed equally to this work.

### Notes

The authors declare no competing financial interest.

## ■ ACKNOWLEDGMENTS

This study was supported by grants from FAPESP (Fundação de Amparo à Pesquisa do Estado de São Paulo), Conselho Nacional de Desenvolvimento Científico e Tecnológico (CNPq), Coordenação de Aperfeiçoamento de Nível Superior - Project NanoBiotec (CAPES), and Biotox Network (CYTED). We are grateful for the help and complementing work of Dr. Malvina Boni-Mitake for the crotonamine purification and also for the illustration figures prepared with the help of Dr. Liza Figueiredo Felicori Vilela (UFMG) and Dr. Vitor Oliveira (UNIFESP).

## ■ ABBREVIATIONS

AMP, antimicrobial peptide; CPP, cell penetrating peptide; ATCC, American Type Culture Collection; MIC, minimal inhibitory concentration; POPG, 1-palmitoyl-2-oleoyl-*sn*-glycero-3-phosphoglycerol; POPC, 1-palmitoyl-2-oleoyl-*sn*-glycero-3-phosphocholine; LUVs, large unilamellar vesicles; GUVs, giant unilamellar vesicles; CF, carboxyfluorescein

## ■ REFERENCES

- (1) Nicastro, G.; Franzoni, L.; Chiara, C.; Mancin, A. C.; Giglio, J. R.; Spisni, A. Solution Structure of Crotonamine, a Na<sup>+</sup> Channel Affecting Toxin from *Crotalus durissus terrificus* Venom. *Eur. J. Biochem.* **2003**, *270*, 1969–1979.
- (2) Fadel, V.; Bettendorff, P.; Herrmann, T.; de Azevedo, W. F., Jr; Oliveira, E. B.; Yamane, T.; Wuthrich, K. Automated NMR Structure Determination and Disulfide Bond Identification of the Myotoxin Crotonamine from *Crotalus durissus terrificus*. *Toxicon* **2005**, *46*, 759–767.
- (3) Coronado, M. A.; Gabdulkhakov, A.; Georgieva, D.; Sankaran, B.; Murakami, M. T.; Arni, R. K.; Betzel, C. Structure of the Polypeptide Crotonamine from the Brazilian Rattlesnake *Crotalus durissus terrificus*. *Acta Crystallogr. D: Biol. Crystallogr.* **2013**, *69*, 1958–1964.
- (4) Rádis-Baptista, G.; Oguiura, N.; Hayashi, M. A.; Camargo, M. E.; Grego, K. F.; Oliveira, E. B.; Yamane, T. Nucleotide Sequence of Crotonamine Isoform Precursors from a Single South American Rattlesnake (*Crotalus durissus terrificus*). *Toxicon* **1999**, *37* (7), 973–984.
- (5) Taylor, K.; Barran, P. E.; Dorin, J. R. Structure-Activity Relationships in Beta-Defensin Peptides. *Biopolymers* **2008**, *90*, 1–7. Review
- (6) Hazlett, L.; Wu, M. Defensins in Innate Immunity. *Cell Tissue Res.* **2011**, *343*, 175–188.
- (7) Kerkis, A.; Hayashi, M. A.; Yamane, T.; Kerkis, I. Properties of Cell Penetrating Peptides (CPPs). *IUBMB Life* **2006**, *58*, 7–13. Review.
- (8) Kerkis, A.; Kerkis, I.; Rádis-Baptista, G.; Oliveira, E. B.; Vianna-Morgante, A. M.; Pereira, L. V.; Yamane, T. Crotonamine Is a Novel Cell-Penetrating Protein from the Venom of Rattlesnake *Crotalus durissus terrificus*. *FASEB J.* **2004**, *18*, 1407–1409.
- (9) Nascimento, F. D.; Sancey, L.; Pereira, A.; Rome, C.; Oliveira, V.; Oliveira, E. B.; Nader, H. B.; Yamane, T.; Kerkis, I.; Tersariol, I. L.; et al. The Natural Cell-Penetrating Peptide Crotonamine Targets Tumor Tissue *in Vivo* and Triggers a Lethal Calcium-Dependent Pathway in Cultured Cells. *Mol. Pharmaceutics* **2012**, *9*, 211–221.
- (10) Yamane, E. S.; Bizerra, F. C.; Oliveira, E. B.; Moreira, J. T.; Rajabi, M.; Nunes, G. L.; de Souza, A. O.; da Silva, I. D.; Yamane, T.; Karpel, R. L.; et al. Unraveling the Antifungal Activity of a South American Rattlesnake Toxin Crotonamine. *Biochimie* **2013**, *95*, 231–240.
- (11) Nascimento, F. D.; Hayashi, M. A.; Kerkis, A.; Oliveira, V.; Oliveira, E. B.; Rádis-Baptista, G.; Nader, H. B.; Yamane, T.; Tersariol, I. L. S.; Kerkis, I. Crotonamine Mediates Gene Delivery into Cells through the Binding to Heparan Sulfate Proteoglycans. *J. Biol. Chem.* **2007**, *282*, 21349–21360.
- (12) Chen, P. C.; Hayashi, M. A.; Oliveira, E. B.; Karpel, R. L. DNA-Interactive Properties of Crotonamine, a Cell-Penetrating Polypeptide and a Potential Drug Carrier. *PLoS One* **2012**, *7*, No. e48913, DOI: 10.1371/journal.pone.0048913.
- (13) Hayashi, M. A.; Oliveira, E. B.; Kerkis, I.; Karpel, R. L. Crotonamine: A Novel Cell-Penetrating Polypeptide Nanocarrier with Potential Anti-Cancer and Biotechnological Applications. *Methods Mol. Biol.* **2012**, *906*, 337–352.
- (14) Hayashi, M. A. F.; Nascimento, F. D.; Kerkis, A.; Oliveira, V.; Oliveira, E. B.; Pereira, A.; Rádis-Baptista, G.; Nader, H. B.; Yamane, T.; Kerkis, I.; et al. Cytotoxic Effects of Crotonamine Are Mediated through Lysosomal Membrane Permeabilization. *Toxicon* **2008**, *52*, 508–517.
- (15) Pereira, A.; Kerkis, A.; Hayashi, M. A.; Pereira, A. S.; Silva, F. S.; Oliveira, E. B.; Prieto da Silva, A. R.; Yamane, T.; Rádis-Baptista, G.; Kerkis, I. Crotonamine Toxicity and Efficacy in Mouse Models of Melanoma. *Expert Opin. Invest. Drugs* **2011**, *20*, 1189–1200.
- (16) Paredes-Gamero, E. J.; Casaes-Rodrigues, R. L.; Moura, G. E.; Domingues, T. M.; Buri, M. V.; Ferreira, V. H.; Trindade, E. S.; Moreno-Ortega, A. J.; Cano-Abad, M. F.; Nader, H. B.; et al. Cell-Permeable Gomesin Peptide Promotes Cell Death by Intracellular Ca(2+) Overload. *Mol. Pharmaceutics* **2012**, *9*, 2686–2697.
- (17) Van Zoggel, H.; Carpentier, G.; Dos Santos, C.; Hamma-Kourbali, Y.; Courty, J.; Amiche, M.; Delbé, J. Antitumor and

Angiostatic Activities of the Antimicrobial Peptide Dermaseptin B2. *PLoS One* **2012**, 7, No. e44351.

(18) Cho, J.; Hwang, I. S.; Choi, H.; Hwang, J. H.; Hwang, J. S.; Lee, D. G. The Novel Biological Action of Antimicrobial Peptides via Apoptosis Induction. *J. Microbiol. Biotechnol.* **2012**, 22, 1457–1466. Review.

(19) Pushpanathan, M.; Gunasekaran, P.; Rajendhran, J. Antimicrobial Peptides: Versatile Biological Properties. *Int. J. Pept.* **2013**, No. 675391.

(20) Song, J.; Zhang, W.; Kai, M.; Chen, J.; Liang, R.; Zheng, X.; Li, G.; Zhang, B.; Wang, K.; Zhang, Y.; et al. Design of an Acid-Activated Antimicrobial Peptide for Tumor Therapy. *Mol. Pharmacol.* **2013**, 10, 2934–2941.

(21) Gaspar, D.; Veiga, A. S.; Castanho, M. A. From Antimicrobial to Anticancer Peptides. A Review. *Front. Microbiol.* **2013**, 4, 294. Review.

(22) Bulet, P.; Stöcklin, R.; Menin, L. Anti-Microbial Peptides: From Invertebrates to Vertebrates. *Immunol. Rev.* **2004**, 198, 169–184.

(23) Jenssen, H.; Hamill, P.; Hancock, R. E. Peptide Antimicrobial Agents. *Clin. Microbiol. Rev.* **2006**, 19, 491–511.

(24) Zasloff, M. Antimicrobial Peptides of Multicellular Organisms. *Nature* **2002**, 415, 389–395.

(25) Yeaman, M. R.; Yount, N. Y. Mechanisms of Antimicrobial Peptide Action and Resistance. *Pharmacol. Rev.* **2003**, 55, 27–55.

(26) Yount, N. Y.; Kupferwasser, D.; Spisni, A.; Dutz, S. M.; Ramjan, Z. H.; Sharma, S.; Waring, A. J.; Yeaman, M. R. Selective Reciprocity in Antimicrobial Activity versus Cytotoxicity of HBD-2 and Crotonamine. *Proc. Natl. Acad. Sci. U.S.A.* **2009**, 106, 14972–14977.

(27) Wimley, W. C.; Hristova, K. Antimicrobial Peptides: Successes, Challenges and Unanswered Questions. *J. Membr. Biol.* **2011**, 239, 27–34.

(28) Whittington, C. M.; Papenfuss, A. T.; Bansal, P.; Torres, A. M.; Wong, E. S.; Deakin, J. E.; Graves, T.; Alsop, A.; Schatzkammer, K.; Kremitzki, C.; et al. Defensins and the Convergent Evolution of Platypus and Reptile Venom Genes. *Genome Res.* **2008**, 18, 986–994.

(29) Oguiura, N.; Boni-Mitake, M.; Rádis-Baptista, G. New View on Crotonamine, a Small Basic Polypeptide Myotoxin from South American Rattlesnake Venom. *Toxicon* **2005**, 46, 363–370. Review.

(30) Oguiura, N.; Boni-Mitake, M.; Affonso, R.; Zhang, G. *In Vitro* Antibacterial and Hemolytic Activities of Crotonamine, a Small Basic Myotoxin from Rattlesnake *Crotalus durissus*. *J. Antibiot.* **2011**, 64, 327–331.

(31) Gonçalves, J. M.; Arantes, E. G. Estudos Sobre Venenos De Serpentes Brasileiras. III. Determinação Quantitativa De Crotonamina No Veneno De Cascavel Brasileira. *An. Acad. Bras. Cienc.* **1956**, 28, 369–371.

(32) Tu, A. T.; Morita, M. Attachment of Rattlesnake Venom Myotoxin A to Sarcoplasmic Reticulum: Peroxidase Conjugated Method. *Br. J. Exp. Pathol.* **1983**, 64, 633–637.

(33) Mebs, D.; Ehrenfeld, M.; Samejima, Y. Local Necrotizing Effect of Snake Venoms on Skin and Muscle: Relationship to Serum Creatine Kinase. *Toxicon* **1978**, 21, 393–398.

(34) Boni-Mitake, M.; Costa, H.; Spencer, P. J.; Vassiliev, V. S.; Rogero, J. R. Effects of 60Co Gamma Radiation on Crotonamine. *Braz. J. Med. Biol. Res.* **2001**, 34, 1531–1538.

(35) Andrushchenko, V. V.; Aarabi, M. H.; Nguyen, L. T.; Prenner, E. J.; Vogel, H. J. Thermodynamics of the Interactions of Tryptophan-Rich Cathelicidin Antimicrobial Peptides with Model and Natural Membranes. *Biochim. Biophys. Acta* **2008**, 1778, 1004–1014.

(36) Sardi, J. C.; Scorzon, L.; Bernardi, T.; Fusco-Almeida, A. M.; Mendes Giannini, M. J. *Candida* Species: Current Epidemiology, Pathogenicity, Biofilm Formation, Natural Antifungal Products and New Therapeutic Options. *J. Med. Microbiol.* **2013**, 62, 10–24.

(37) Ralston, E.; Hjelmeland, L. M.; Klausner, R. D.; Weinstein, J. N.; Blumenthal, R. Carboxyfluorescein as a Probe for Liposome-Cell Interactions. Effect of Impurities and Purification of the Dye. *Biochim. Biophys. Acta* **1981**, 649, 133–137.

(38) Rouser, G.; Fkeischer, S.; Yamamoto, A. Two Dimensional then Layer Chromatographic Separation of Polar Lipids and Determination

of Phospholipids by Phosphorus Analysis of Spots. *Lipids* **1970**, 5, 494–496.

(39) Domingues, T. M.; Mattei, B.; Seelig, J.; Perez, K. R.; Miranda, A.; Riske, K. A. Interaction of the Antimicrobial Peptide Gomesin with Model Membranes: A Calorimetric Study. *Langmuir* **2013**, 29, 8609–8618.

(40) Shin, J. H.; Kee, S. J.; Shin, M. G.; Kim, S. H.; Shin, D. H.; Lee, S. K.; Suh, S. P.; Ryang, D. W. Biofilm Production by Isolates of *Candida* Species Recovered from Nonneutropenic Patients: Comparison of Bloodstream Isolates with Isolates from Other Sources. *J. Clin. Microbiol.* **2002**, 40, 1244–1248.

(41) Ramage, G.; VandeWalle, K.; Wickes, B. L.; López-Ribot, J. L. Biofilm Formation by *Candida dubliniensis*. *J. Clin. Microbiol.* **2001**, 39, 3234–3240.

(42) Mally, M.; Majhenc, J.; Svetina, S.; Zeks, B. The Response of Giant Phospholipid Vesicles to Pore-Forming Peptide Melittin. *Biochim. Biophys. Acta* **2007**, 1768, 1179–1189.

(43) Tamba, Y.; Yamazaki, M. Single Giant Unilamellar Vesicle Method Reveals Effect of Antimicrobial Peptide Magainin 2 on Membrane Permeability. *Biochemistry* **2005**, 44, 15823–15833.

(44) Ros, U.; Pedrera, L.; Diaz, D.; Karam, J. C.; Sudbrack, T. P.; Valiente, P. A.; Martínez, D.; Cilli, E. M.; Pazos, F.; Itri, R.; et al. The Membranotropic Activity of N-Terminal Peptides from the Pore-Forming Proteins Sticholysin I and II Is Modulated by Hydrophobic and Electrostatic Interactions as Well as Lipid Composition. *J. Biosci.* **2011**, 36, 781–791.

(45) Taff, H. T.; Mitchell, K. F.; Edward, J. A.; Andes, D. R. Mechanisms of *Candida* Biofilm Drug Resistance. *Future Microbiol.* **2013**, 8, 1325–1337.

(46) Singh, A.; Prasad, T.; Kapoor, K.; Mandal, A.; Roth, M.; Welti, R.; Prasad, R. Phospholipidome of *Candida*: Each Species of *Candida* Has Distinctive Phospholipid Molecular Species. *OMICS* **2010**, 14 (6), 665–677.

(47) Domingues, T. M.; Riske, K. A.; Miranda, A. Revealing the Lytic Mechanism of the Antimicrobial Peptide Gomesin by Observing Giant Unilamellar Vesicles. *Langmuir* **2010**, 26, 11077–11084.

(48) Sudbrack, T. P.; Archilha, N. L.; Itri, R.; Riske, K. A. Observing the Solubilization of Lipid Bilayers by Detergents with Optical Microscopy of GUVs. *J. Phys. Chem. B* **2011**, 115, 269–277.

(49) Sieber, M.; Bosch, B.; Hanke, W.; Fernandes de Lima, V. M. Membrane-Modifying Properties of Crotonamine, a Small Peptide-Toxin from *Crotalus durissus terifficus* Venom. *Biochim. Biophys. Acta* **2013**, S0304–4165, 471–476.

(50) Wadhvani, P.; Epand, R. F.; Heidenreich, N.; Bürck, J.; Ulrich, A. S.; Epand, R. M. Membrane-Active Peptides and the Clustering of Anionic Lipids. *Biophys. J.* **2012**, 103, 265–274.

(51) Lourenzoni, M. R.; Namba, A. M.; Caseli, L.; Degre, L.; Zaniquelli, M. E. Study of the Interaction of Human Defensins with Cell Membrane Models: Relationships between Structure and Biological Activity. *J. Phys. Chem. B* **2007**, 111, 11318–11329.

(52) Hoover, D. M.; Rajashankar, K. R.; Blumenthal, R.; Puri, A.; Oppenheim, J. J.; Chertov, O.; Lubkowski, J. The Structure of Human B-Defensin-2 Shows Evidence of Higher Order Oligomerization. *J. Biol. Chem.* **2000**, 275, 32911–32918.

(53) Hoover, D. M.; Chertov, O.; Lubkowski, J. The Structure of Human B-Defensin-1. *J. Biol. Chem.* **2001**, 276, 39021–39026.

(54) Vazdar, M.; Wernersson, E.; Khabiri, M.; Cwiklik, L.; Jurkiewicz, P.; Hof, M.; Mann, E.; Kolusheva, S.; Jelinek, R.; Jungwirth, P. Aggregation of Oligoarginines at Phospholipid Membranes: Molecular Dynamics Simulations, Time-Dependent Fluorescence Shift, and Biomimetic Colorimetric Assays. *J. Phys. Chem. B* **2013**, 117 (39), 11530–11540.

(55) Beltran, J. R.; Mascarenhas, Y. P.; Craievich, A. F.; Laure, C. J. SAXS Study of Structure and Conformational Changes of Crotonamine. *Biophys. J.* **1985**, 47, 33–35.

(56) Hampe, O. G.; Junqueira, N. O.; Vozari-Hampe, M. M. Polyacrylamide Gel Electrophoretic Studies on the Self Association of Crotonamine: Characterization and Molecular Dimension of N-Mer Species. *Electrophoresis* **1990**, 11, 475–478.



- (57) Mago, N.; Khuller, G. K. Lipids of *Candida albicans*: Subcellular Distribution and Biosynthesis. *J. Gen. Microbiol.* **1990**, *136*, 993–996.
- (58) Cerbón, J.; Calderón, V. Surface Potential Regulation of Phospholipid Composition and In-Out Translocation in Yeast. *Eur. J. Biochem.* **1994**, *219*, 195–200.
- (59) Abdi, M.; Drucker, D. B. Phospholipid Profiles in the Oral Yeast *Candida*. *Arch. Oral Biol.* **1996**, *41*, 517–522.
- (60) Iñigo, M.; Pemán, J.; Del Pozo, J. L. Antifungal Activity against *Candida* Biofilms. *Int. J. Artif. Organs* **2012**, *35*, 780–791.
- (61) Bonhomme, J.; d'Enfert, C. *Candida albicans* Biofilms: Building a Heterogeneous, Drug-Tolerant Environment. *Curr. Opin. Microbiol.* **2013**, *16*, 398–403.
- (62) Donlan, R. M.; Costerton, J. W. Biofilms: Survival Mechanisms of Clinically Relevant Microorganisms. *Clin. Microbiol. Rev.* **2002**, *15*, 167–193.
- (63) Ferreira, A. V.; Prado, C. G.; Carvalho, R. R.; Dias, K. S.; Dias, A. L. *Candida albicans* and non-*C. albicans* *Candida* Species: Comparison of Biofilm Production and Metabolic Activity in Biofilms, and Putative Virulence Properties of Isolates from Hospital Environments and Infections. *Mycopathologia* **2013**, *175*, 265–272.
- (64) Lattif, A. A.; Mukherjee, P. K.; Chandra, J.; Roth, M. R.; Welti, R.; Rouabhia, M.; Ghannoum, M. A. Lipidomics of *Candida albicans* Biofilms Reveals Phase-Dependent Production of Phospholipid Molecular Classes and Role for Lipid Rafts in Biofilm Formation. *Microbiology* **2011**, *157*, 3232–3242.
- (65) Rodrigues, M.; Santos, A.; de la Torre, B. G.; Rádis-Baptista, G.; Andreu, D.; Santos, N. C. Molecular Characterization of the Interaction of Crotamine-Derived Nucleolar Targeting Peptides with Lipid Membranes. *Biochim. Biophys. Acta* **2012**, *1818*, 2707–2717.

#### ■ NOTE ADDED AFTER ASAP PUBLICATION

This paper was published ASAP on May 7, 2014. The abstract graphic was updated. The revised paper was reposted on May 9, 2014.